

# Strange quark production in a statistical effective model

F. Becattini and G. Pettini

*Department of Physics, University of Florence and INFN Sezione di Firenze  
Via G. Sansone 1, I-50109, Sesto F.no, Firenze, Italy\**

An effective model with constituent quarks as fundamental degrees of freedom is used to predict the relative strangeness production pattern in both high energy elementary and heavy ion collisions. The basic picture is that of the statistical hadronization model, with hadronizing color-singlet clusters assumed to be at full chemical equilibrium at constituent quark level. Thus, by assuming that at least the ratio between strange and non-strange constituent quarks survives in the final hadrons, the apparent undersaturation of strange particle phase space observed in the data can be accounted for. In this framework, the enhancement of relative strangeness production in heavy ion collisions in comparison with elementary collisions is mainly owing to the excess of initial non-strange matter over antimatter and the so-called canonical suppression, namely the constraint of exact color and flavor conservation over small volumes.

## I. INTRODUCTION

The recent observation that hadron multiplicities in  $e^+e^-$  and hadronic high energy collisions agree very well with a statistical-thermodynamical ansatz [1, 2] has revived the interest on the statistical models in high energy collisions, an idea dating back to the 50's [3, 4]. As the apparent chemical equilibrium of all hadron species in these elementary collisions (EC) cannot be driven by inelastic collisions amongst hadrons after their formation, this finding has led to the idea of a pure statistical filling of multi-hadronic phase space of homogeneous hadronizing regions (*clusters* or *fireballs*) as an intrinsic feature of hadronization process, occurring at a critical value of energy density [2, 5, 6]. Otherwise stated, hadrons are born in an equilibrium state, as envisaged by Hagedorn [7]. It must be emphasized that, within this framework, temperature and other thermodynamical quantities have an essential statistical meaning which does not imply the occurrence of a thermalization process via inelastic hadronic collisions.

The same model, in different versions, has been successfully applied to a large set of heavy ion collisions (HIC) data [8, 9, 10] and this has been interpreted as a clue of the minor effect of post-hadronization inelastic rescattering [5], an indication which is also supported by kinetic models calculations [11].

One of the nice features of the statistical hadronization model (SHM) is the very low number of free parameters required to reproduce a large number of hadronic multiplicities. Provided that the masses and charges of the assumed hadronizing clusters fluctuate according to a particular shape function [2, 12], all Lorentz-invariant quantities (like e.g. hadron average multiplicities) depend on two parameters: the sum  $V$  of the volumes of the clusters and the temperature  $T$ . However, in order to get a satisfactory agreement with the data, the model has to be supplemented, both in EC and HIC, with one more phenomenological parameter,  $\gamma_S$ , suppressing the production of particles containing  $n$  strange valence quarks by  $\gamma_S^n$  with respect to the expected production in a fully equilibrated hadron gas <sup>1</sup>.

The behavior of  $\gamma_S$  as a function of collision and center-of-mass energy was found to be rather odd as it turns out to be significantly higher in  $e^+e^-$  collisions than in hadronic collisions over a large energy range [1, 2] whereas it has a fairly stable value in heavy ion collisions [9], which is approximately the same as in  $e^+e^-$  collisions. A clearer insight in the mechanism of strangeness production can be achieved by estimating the ratio between newly produced valence strange and up, down quark pairs, the so-called Wroblewski factor  $\lambda_S$ :

$$\lambda_S = \frac{2\langle s\bar{s} \rangle}{\langle u\bar{u} \rangle + \langle d\bar{d} \rangle} \quad (1)$$

which shows a striking regularity, being in fact fairly constant in all kinds of elementary collisions [10] over two orders of magnitude of center-of-mass energy and as twice as large in high energy heavy ion collisions (see Fig. 1). It should be stressed that this ratio is calculated by counting the *primarily* produced quark pairs, i.e. those belonging to directly emitted hadrons. As primary hadrons are not measurable, they must be calculated by using a model and  $\lambda_S$  turns out to be a model dependent quantity especially with regard to the number of u and d quarks which significantly

---

\*Electronic address: becattini@fi.infn.it, pettini@fi.infn.it

<sup>1</sup> Recently, a different parameterization of the extra strangeness suppression has been introduced for elementary collisions [12].

increases during the post-hadronization hadronic decay chain. However, if the number of measured species is large and the model accurately reproduces them (which is the case for the SHM), the thereby estimated  $\lambda_S$  is expected to be reasonably close to the actual value. The need of an extra suppression of strangeness with respect to the full statistical equilibrium for the hadronic system urges the search for an explanation based on a more microscopic approach. This is indeed the main subject of the present work, where we try to calculate  $\lambda_S$  within one statistical model scheme in both EC and HIC, employing a constituent quark model as the basic underlying structure, with the purpose of justifying the lack of strangeness chemical equilibrium at hadron level observed in the data. In fact, constituent quark models have already been used to calculate strangeness production in HIC on the basis of transport equation [13]. Amongst other microscopic approaches to this problem and, more generally, to account for hadronization equilibrium features, a recent study has been performed in ref. [14] focussed on the role of massive Polyakov loops.

The paper is organized as follows: in Sect. II we introduce the physical picture and in Sect. III the full model is described. In Sect. IV the Nambu-Jona-Lasinio model with exact conservation of quantum charges is used to calculate  $\lambda_S$  and compare it with the corresponding value obtained from fits of the statistical hadronization model to the data in both HIC and EC. Also, the stability of the results is addressed. Sect. V is devoted to conclusions.

## II. THE PHYSICAL PICTURE

The physical picture keeps the same scheme of the SHM: formation of a set of clusters endowed with charge, momentum, mass and volume, in local statistical equilibrium. However, statistical equilibrium is now assumed to apply to a system of constituent quarks whilst hadrons are assumed to be produced via their coalescence, still in a purely statistical fashion (*statistical coalescence*) so as to give rise to a *partially* chemically equilibrated hadron gas. Furthermore, each cluster is required to be a color singlet. This requirement has of course no effect at hadron level, but it is crucial in a quark model.

Two more crucial assumptions are introduced. First, the thermodynamical parameters fitted in the SHM, in high energy EC and HIC, are interpreted as the critical values for color deconfinement and, consequently, for (approximate) chiral symmetry restoration [15, 16]; secondly, it is assumed that the produced s and light quarks, or at least the ratio s/u, i.e.  $\lambda_S$ , survive in the final hadrons after hadronization has taken place.

The first assumption is supported by the constancy of the fitted temperatures in the SHM for various processes in EC [17] and by its agreement with other estimates of the critical temperature; in view of this fact, the use of effective models such as the Nambu-Jona-Lasinio model [18, 19] and others [20, 21, 22, 23] embodying chiral symmetry breaking and restoration, looks well suited. It should be pointed out that the values of the thermodynamical parameters (i.e. temperature and baryon-chemical potentials) extracted within the SHM in HIC (see Table I) lie in a range where all effective models and recent lattice simulations [24] predict smooth cross-over transitions, far from a possible critical ending point. For the same reason, extensions of the NJL model [25, 26] at high baryon chemical potential and low temperature, where color superconductivity takes place[27], can be disregarded.

The second assumption allows us to calculate  $\lambda_S$  within a quark model and compare it with that obtained from valence quark counting in the produced hadrons. Also, it implies that the lack of full chemical equilibrium at hadron level is indeed the consequence of full chemical equilibrium at constituent quark level.

In the grand-canonical framework, which applies to a large system,  $\lambda_S$  would depend only on intensive quantities such as chemical potentials and temperature and its constancy would be tightly related to theirs. However, if the system is not large, the canonical (and possibly micro-canonical) ensemble, in which the exact conservation of cluster quantum numbers in the hadronic or quark system is enforced, must be used and, as a consequence,  $\lambda_S$  gets a dependence also on the volume (the so-called *canonical suppression*). While the volume within which quantum charges (baryon number, electric charge and strangeness) are fixed can be taken as the sum of the proper volumes of all clusters, though under appropriate non-trivial assumptions [2, 12], the volume over which color must be neutralized is, as has been mentioned, that of a single hadronizing cluster. This very fact introduces a further parameter in the model, i.e. the average single cluster volume  $V_c$  which can indeed be much smaller than the volume over which flavor is conserved. As quarks do carry color charge,  $\lambda_S$  might be significantly affected by variations of  $V_c$ .

Therefore, the underlying idea is that the presence of a characteristic constant value of  $V_c$  in EC, related to the typical distance over which color is neutralized, may sizeably reduce the value of  $\lambda_S$  (together with flavor constraint) whereas color deconfinement in HIC may lead to an enhancement of s/u ratio. We thus argue that the main difference between hadronization in EC and HIC is to be found in the typical size of the pre-hadronization color-neutral region: it has to be something of the order of a hadron radius in EC (a sort of mini-QGP droplet) and much larger in HIC if a macroscopic (i.e. extending over many hadron volumes) QGP has been formed. Of course, it must be emphasized that the process stage at which the statistical equilibrium is achieved is expected to be deeply different in EC as compared with HIC: an *early* thermalization of partons is indeed envisaged in HIC, which is maintained until hadronization, whereas a *late*, pre-hadronization local equilibrium scenario, possibly driven by the strongly coupled

non-linear evolution of QCD fields in the late soft regime is envisaged for EC.

Hence, we argue that relative strange quark production might probe these two scenarios because of a possible stronger color and flavor-canonical suppression of s quarks with respect to u and d quarks in EC which is absent in HIC due to much larger single-cluster volume and overall volume. The ultimate reason of the stronger canonical suppression of s quarks in comparison with u, d, resides in their different constituent mass values. The hereby proposed mechanism of strangeness enhancement in HIC is rather different from that suggested by Muller and Rafelski [28] insofar as no difference in the time scale is invoked but an equilibrium situation is assumed in both EC and HIC, though over differently sized regions.

### III. THE MODEL

According to the basic idea of the SHM and what has been said in the previous section, the formation of a set of pre-hadronic, color-singlet clusters at statistical equilibrium, with definite values of flavor quantum numbers is envisaged as the result of a complex dynamical evolution. In an equilibrium scheme, all physical observables relevant to a particular cluster can be calculated by means of suitable operations on its associated partition function. Provided that cluster masses are large enough so that micro-canonical effects can be neglected, the requirement of definite quantum numbers implies that the  $i^{\text{th}}$  cluster's partition function has to be the *canonical* one rather than the more familiar grand-canonical:

$$Z_i = \sum_{\text{states}} e^{-E/T} \quad (2)$$

where  $T$  is the cluster's temperature,  $E$  its energy and the sum is meant to run over all *allowed* states, namely the states with flavor and color quantum numbers matching those of the cluster. The calculation of  $Z_i$  can be done by using the symmetry group  $G$  associated to the involved quantum numbers. If the *continuous* group  $G$  is an exact internal symmetry for the Hamiltonian  $H$  and the cluster state belongs to its irreducible representation  $\nu$ , then [29]:

$$Z_i = \int d\mu(\gamma_1, \dots, \gamma_r) \chi_\nu^*(\gamma_1, \dots, \gamma_r) \hat{Z}_i(\gamma_1, \dots, \gamma_r) = \int d\mu(\gamma_1, \dots, \gamma_r) \chi_\nu^*(\gamma_1, \dots, \gamma_r) \text{Tr} \left( e^{-\beta H - 1 \sum_{l=1}^r \gamma_l Q_l} \right) \quad (3)$$

where  $d\mu(\gamma_1, \dots, \gamma_r)$  is the invariant normalized measure of  $G$ ,  $\chi_\nu$  is the character of the representation  $\nu$ ,  $r$  is the rank of  $G$ ,  $Q_l$  are the mutually commuting generators of the Cartan subalgebra and  $\gamma_l$  are the group parameters. The actual group of interest is  $\text{SU}(3) \times \text{U}(1)^3$ , where each  $\text{U}(1)$  corresponds to conserved net flavors  $U$ ,  $D$  and  $S$  and  $\text{SU}(3)$  to the color. For instance, the canonical partition function of the  $i^{\text{th}}$  cluster of a gas of free quarks (no antiquarks included) with flavor  $j$  involves the following  $\hat{Z}_i$  in Eq. (3):

$$\hat{Z}_i(\theta_1, \theta_2, \phi_j) = \exp \left( \sum_{n=1}^{\infty} \frac{(-1)^{n+1}}{n} \chi_{1,0}(n\theta_1, n\theta_2) e^{1n\phi_j} \frac{gV}{(2\pi)^3} \int d^3p e^{-\frac{n\epsilon_j}{T}} \right) \quad (4)$$

where:

$$\chi_{1,0}(\theta_1, \theta_2) = e^{-1\theta_1} + e^{-1\theta_2} + e^{1(\theta_1 + \theta_2)} \quad (5)$$

is the character of the fundamental representation of  $\text{SU}(3)$ , with  $\theta_{1,2} \in [-\pi, \pi]$ ;  $\phi_j$  is the parameter of  $\text{U}(1)_j$   $V$  is the volume,  $g$  is the spin degeneracy factor,  $\epsilon_j = \sqrt{p^2 + m_j^2}$  and the sum over discrete states  $k$  has been approximated with its continuum limit. When including antiquarks and considering three flavors (i.e. the full group  $\text{SU}(3) \times \text{U}_u(1) \times \text{U}_d(1) \times \text{U}_s(1)$ ),  $\hat{Z}^i$  can be written as the product of three functions like those in Eq. (4):

$$\hat{Z}^i(\theta_1, \theta_2, \phi_u, \phi_d, \phi_s) = \prod_{j=u,d,s} \hat{Z}_{ij}(\theta_1, \theta_2, \phi_j) \hat{Z}_{ij}^*(\theta_1, \theta_2, \phi_j) \quad (6)$$

The irreducible representation  $\nu$  can be labelled by three integer numbers, the net flavor  $U_i, D_i, S_i$ , and, as far as the  $\text{SU}(3)$  color group is concerned,  $\nu$  is simply the singlet representation. Therefore, by introducing the vectors  $\mathbf{Q}_i = (U_i, D_i, S_i)$  and  $\phi_i = (\phi_{iU}, \phi_{iD}, \phi_{iS})$ , the character can be written as  $\chi_\nu = \exp[-1\mathbf{Q}_i \cdot \phi_i]$  and:

$$Z_{ij} = \left[ \prod_{j=1}^3 \int_{-\pi}^{\pi} \frac{d\phi_j}{2\pi} \right] \int d\mu(\theta_1, \theta_2) e^{1\mathbf{Q}_i \cdot \phi_i} \hat{Z}_i(\theta_1, \theta_2, \phi_i) \quad (7)$$

where:

$$\int d\mu(\theta_1, \theta_2) = \frac{1}{3!} \int_{-\pi}^{\pi} \frac{d\theta_1}{2\pi} \int_{-\pi}^{\pi} \frac{d\theta_2}{2\pi} \prod_{j < k}^3 4 \sin^2 \frac{\theta_j - \theta_k}{2} \quad (8)$$

with the constraint  $\sum_{k=1}^3 \theta_k = 0 \pmod{2\pi}$ , is the  $SU(3)$  invariant integration. The partition function hitherto considered is relevant to one cluster. Yet, there are several clusters in a single collision event and, as long as global observables are concerned, theoretical predictions require summation over all clusters. Moreover, clusters may well be produced with different configurations of flavor numbers  $(U_i, D_i, S_i)$  in different events (provided that their sum fulfills the conservation law, i.e. it must be equal to the flavor numbers of the colliding particles), hence an integration over all possible configurations weighted by its probability must be carried out in order to calculate averages of physical quantities. However, the probability distribution of clusters flavor configuration is an unknown function, which cannot be predicted within the statistical model and which is most likely governed by the preceding dynamical process. We will therefore assume a configuration probability distribution  $w$  which is the ‘‘maximum disorder’’ one and which allows a remarkable simplification of the expressions of averages quark multiplicities as well as any other Lorentz-invariant observables. This function  $w$ , for an event with  $N$  clusters can be written as:

$$w(\mathbf{Q}_1, \dots, \mathbf{Q}_N) = \frac{\prod_{i=1}^N Z_i(\mathbf{Q}_i) \delta_{\mathbf{Q}, \Sigma_i \mathbf{Q}_i}}{\sum_{\mathbf{Q}_1, \dots, \mathbf{Q}_N} \prod_{i=1}^N Z_i(\mathbf{Q}_i) \delta_{\mathbf{Q}, \Sigma_i \mathbf{Q}_i}} \quad (9)$$

where  $Z_i$  as in Eq. (7), the  $\delta$  ensures that global conservation of initial quantum numbers  $\mathbf{Q}$  is fulfilled. If one has to calculate the average multiplicity of a given quark species  $j$  in a  $N$  cluster event, it is advantageous to introduce a fictitious fugacity  $\lambda_j$  and taking the derivative of  $\log Z_i$  with respect to it, so that the overall multiplicity reads:

$$\begin{aligned} \langle n_j \rangle &= \sum_{\mathbf{Q}_1, \dots, \mathbf{Q}_N} w(\mathbf{Q}_1, \dots, \mathbf{Q}_N) \sum_{i=1}^N \frac{\partial}{\partial \lambda_j} \log Z_i(\mathbf{Q}_i) \Big|_{\lambda_j=1} = \\ &= \sum_{\mathbf{Q}_1, \dots, \mathbf{Q}_N} w(\mathbf{Q}_1, \dots, \mathbf{Q}_N) \frac{\partial}{\partial \lambda_j} \prod_{i=1}^N \log Z_i(\mathbf{Q}_i) \Big|_{\lambda_j=1} \end{aligned} \quad (10)$$

and, by using Eq. (9):

$$\langle n_j \rangle = \frac{\partial}{\partial \lambda_j} \log \sum_{\mathbf{Q}_1, \dots, \mathbf{Q}_N} \prod_{i=1}^N Z_i(\mathbf{Q}_i) \delta_{\mathbf{Q}, \Sigma_i \mathbf{Q}_i} \Big|_{\lambda_j=1} \quad (11)$$

Were not for the color-singlet constraint stuck to each  $Z_i$ , the sum over all configurations on the right hand side of Eq. (11) would be, for  $\lambda_j = 1$ , the canonical partition function of a single cluster having as volume the sum of volumes of the individual clusters and with quantum number vector  $\mathbf{Q}$  [2], provided that all clusters have the same temperature. Thereby, also the explicit dependence on  $N$  would vanish. However, this is no longer true once the color singlet constraint is introduced. For a similar strong equivalence with one cluster to apply, single clusters should be in suitable color quantum states superpositions, which is definitely against the common belief of pre-confinement and local color neutralization. Nevertheless, it can be proved that a considerable simplification in Eq. (11) occurs if clusters in one event are assumed to have the same volume, i.e.  $V_i \equiv V_c$ . In that case, it can be proved (see Appendix A) that the right hand side of Eq. (11), which can be defined as the *global partition function*, reads:

$$Z = \left[ \prod_{j=1}^3 \int_{-\pi}^{\pi} \frac{d\phi_j}{2\pi} \right] e^{i\mathbf{Q} \cdot \phi} \left[ \int d\mu(\theta_1, \theta_2) \hat{Z}_i(\theta_1, \theta_2, \phi) \right]^{V/V_c} \quad (12)$$

where  $V = \sum_i V_i = NV_c$  (for the free quarks gas  $\hat{Z}_i$  is given by Eq. (6) with the single flavor term  $\hat{Z}_{ij}(\theta_1, \theta_2, \phi_j)$  calculated from Eq. (4) with (5)). The introduction of the local color-singlet constraint gets the value of the global partition function severely reduced with respect to an only *globally* color-singlet constrained case where clusters are allowed to be in a quantum superposition of colored states. This can be quite easily understood for any extra constraint essentially involves a decrease of the number of available states in the system. If  $V_c \equiv V$  and  $V$  is very large, i.e. in the thermodynamical limit, it can be shown that the usual grand-canonical expressions of the partition function, average multiplicities etc. are recovered.

Besides the basic assumption of local statistical equilibrium (for a single cluster), the expression (12) ultimately relies on a particular choice of flavor distribution (i.e. (9)) among clusters, which is indeed a non-trivial assumption. This particular distribution allows the reduction to one equivalent global cluster just because it is the “maximum disorder” distribution, namely the probability of obtaining a configuration  $(\mathbf{Q}_1, \dots, \mathbf{Q}_N)$  by randomly splitting a statistically equilibrated global cluster into  $N$  sub-cluster each with volume  $V_c$  and in a color singlet state ; in fact, this can be proved by showing that the  $w$ 's in Eq. (9) minimize the free energy of the system (see Appendix B).

It should be pointed out that hadronizing clusters might be too small for a local (i.e. in each of them) temperature to be defined, as we have tacitly assumed. Should this be the case, the appropriate treatment would be micro-canonical and not canonical, with clusters described by mass and volume instead of temperature and volume. Notwithstanding, as far as the calculation of Lorentz-invariants is concerned, a global temperature may still be recovered by resorting to a similar equivalent global cluster reduction procedure at micro-canonical level, which is described in detail in ref. [12]<sup>2</sup>, with a micro-canonical equivalent of the distribution (9). The proof is quite lengthy and the mathematical framework more involved, but it is no longer necessary to assume that each cluster ought to have the same temperature. In fact, only the equivalent global cluster or, equivalently, the global canonical partition function (12), must be large enough to allow a canonical treatment of the system as a whole.

We now have to face the problem of a suitable choice of a microscopic Hamiltonian to be used in Eq. (3) and, thereby, make a theoretical calculation of  $\lambda_S$ . As full QCD is out of question, we resort to QCD-inspired low energy models. The simplest model to start with is the Nambu-Jona-Lasinio (NJL) model, which has quarks as fundamental degrees of freedom and embodies essential features of dynamical chiral symmetry breaking ( $\chi$ SB) in the limit of vanishing current quark masses. Also, we confine ourselves to mean-field approximation, as presented in ref. [19], using the effective Hamiltonian:

$$H_{MFA}^{NJL} = V [g_s(\alpha^2 + \beta^2 + \gamma^2) + 4g_D\alpha\beta\gamma] + \int d^3x \bar{q}(-i\boldsymbol{\gamma} \cdot \nabla + \mathbf{M})q \quad (13)$$

where  $V$  is the spatial volume,  $g_s$  and  $g_D$  are the four-fermion and the six-fermion  $U(1)_A$ -breaking couplings respectively [19, 30],  $\alpha = \langle \bar{u}u \rangle$ ,  $\beta = \langle \bar{d}d \rangle$ ,  $\gamma = \langle \bar{s}s \rangle$  are the quark condensates and:

$$\begin{aligned} M_u &= m_u - 2g_s\alpha - 2g_D\beta\gamma \\ M_d &= m_d - 2g_s\beta - 2g_D\alpha\gamma \\ M_s &= m_s - 2g_s\gamma - 2g_D\alpha\beta \end{aligned} \quad (14)$$

are the constituent quark masses which, owing to the contact four-fermion interaction, are linearly related to the current quark masses  $m_u, m_d, m_s$ . As far as the grand-canonical calculation is concerned, the variational parameters  $\alpha, \beta, \gamma$  are determined by minimizing the effective potential [19] obtained within standard methods [31, 32]. Of course, the same result can be readily obtained by calculating:

$$\begin{aligned} Z &= \text{Tr} e^{-\beta \left( H - \sum_i \mu_j \hat{N}_j \right)} \\ &= e^{-\Gamma|_{\min}} \end{aligned} \quad (15)$$

with  $H = H_{MFA}^{NJL}$ . In Eq. (15),  $\hat{N}_j$  are the conserved flavor operators and  $\Gamma|_{\min}$  is the effective action at the physical point. For constant fields  $\Gamma|_{\min} = \beta V \mathcal{V}|_{\min} = -\log Z$ , where  $\mathcal{V}$  is the effective potential.

The quark over antiquark excess is obtained by taking the derivative of  $\mathcal{V}$  with respect to the chemical potential for a given flavor:

$$\langle n_j - \bar{n}_j \rangle = -\frac{\partial \mathcal{V}|_{\min}}{\partial \mu_j} \quad (16)$$

whereas the number of particles, in the grand-canonical ensemble, reads:

$$\langle n_j \rangle = \frac{N_c V}{\pi^2} \int_0^\Lambda dp \frac{p^2}{e^{\beta \left( \sqrt{p^2 + M_j^2} - \mu_j \right)} + 1} \quad (17)$$

---

<sup>2</sup> Therein, the proof has been given for a hadron gas but it can be easily extended to the present case.

where  $\Lambda$  is an UV cutoff and  $N_c$  the number of colors.

One of the remarkable features of the Hamiltonian  $H_{MFA}^{NJL}$  in Eq. (13) is that the previously obtained expressions in Eqs. (7), (12) for the free quark gas partition functions with exact flavor and color conservation, can be taken up by simply replacing the current masses with the constituent masses  $m_j \rightarrow M_j$  and setting the cutoff  $\Lambda$  as upper bound for the momentum integration in Eq. (4).

The NJL model is the simplest choice in order to study strange quark production, yet it is not a compelling one. Actually, its validity is limited within a temperature range well below the UV cutoff  $\Lambda$  [26]. However, we are reasonably confident that the main results found within this model would not essentially change when employing other effective models whose validity, in principle, extend to arbitrarily high temperatures. As an example, it is worth mentioning the model developed in refs. [20, 21, 22], named in ref. [19] as *ladder-QCD*. In this model the exchange of a gauge particle between quarks is considered, implying a momentum dependence of the self-energy and, consequently, an irreducibility to a simple model with free constituent quarks as in NJL. However, *ladder-QCD* is considerably different from NJL only in the UV regime, where a  $1/p^2$  tail is added to the self-energy, which is otherwise constant in the small momentum region [20, 33]. The effect of the different behaviour in the UV regime on the integrated number of particles is expected to be rather small [20].

#### IV. ANALYSIS AND RESULTS

The goal of the numerical analysis is the calculation of  $\lambda_S$  in both HIC and EC, by performing the ratio between newly produced strange quark and u, d quark pairs in the NJL model. The main ingredient needed to calculate  $\lambda_S$  are the constituent quark masses which, for a given temperature and baryon-chemical potential, have to be determined by the minimization of the free energy  $F$  and thus depend on the parameters contained in the effective Hamiltonian (13), i.e.  $g_S$ ,  $\Lambda$ ,  $g_D$  and the current quark masses. Their values have been fitted at zero temperature and baryon density in ref. [19] to many static and dynamical meson properties:

$$\begin{aligned} \hat{m} &= \frac{m_u + m_d}{2} = 5.5 \text{ MeV}; & m_s &= 135.7 \text{ MeV} \\ \Lambda &= 631.4 \text{ MeV}; & g_S \Lambda^2 &= 3.67; & g_D \Lambda^5 &= -9.29 \end{aligned} \quad (18)$$

Particularly for  $g_D$ , in ref. [19] a temperature dependence is introduced through the phenomenological law:

$$g_D(T) = g_D(T=0) e^{-(T/T_0)^2} \quad (19)$$

where  $T_0$  is a further free parameter and  $g_D(T=0)$  is quoted in Eq. (18). Different values of  $T_0$  give rise to different behaviors of the constituent u, d mass (see Fig. 2 later on) as a function of the temperature as well as different positions of the cross-over curve in the  $(\mu_B, T)$  plane. According to the statement in Sect. II, we take the thermodynamical parameters  $T$  and  $\mu_B$  in Table I as an input, and therefore  $T_0$  can be fixed by enforcing that the quark susceptibility for a light quark with mass  $\hat{m}$  in Eq. (18):

$$\chi_m = \left. \frac{\partial \langle \bar{u}u \rangle}{\partial m} \right|_{m=\hat{m}} \quad (20)$$

has a peak at the desired  $(\mu_B, T)$  point. This has been done for the most accurately determined thermodynamical parameters, which are those in Pb-Pb collisions at  $\sqrt{s_{NN}} = 17.3$  GeV, yielding  $T_0 = 170$  MeV (see Fig. 3). Thereby, all relevant parameters are now fixed. The only free parameter left is the single cluster proper volume  $V_c$ , which may vary as a function of center-of-mass energy and colliding system. The dependence of  $\lambda_S$  on this parameter is a crucial issue to be studied because it can possibly establish a relationship between color deconfinement and strangeness enhancement.

##### A. Heavy Ions

In HIC, calculations are much simpler as the total volumes (namely the sum of proper volumes of all the clusters) turn out to be so large that the effect of the canonical suppression related to exact conservation of flavor quantum numbers can be disregarded [34], provided that flavor quantum numbers are distributed among clusters according to

the function (9). Indeed, it should be pointed out that different scenarios have been devised in which the volume within which strangeness exactly vanishes (*strangeness correlation volume*) is less than the total volume, but this approach cannot account for the low yield of  $\phi$  meson [35], so we will stick to the identification between the strangeness correlation volume and the total volume. If  $V_c$  is large enough, quark multiplicities can thus be estimated by means of Eq. (17), the grand-canonical formula, and  $\lambda_S$  turns out to be independent of  $V$ . In fact, it must be emphasized that the total volumes fitted in the SHM for HIC, though affected by large errors, lie in a range (see Table I) where canonical suppression is negligible and  $\lambda_S$  is sensitive to  $V_c$  if this is roughly below  $10 \text{ fm}^3$  (see Fig. 4). This little sensitivity to  $V_c$  makes  $\lambda_S$  certainly not a clear-cut probe for deconfinement, though hadronizing clusters as small as some  $\text{fm}^3$  can indeed be excluded.

Hence, by taking a full grand-canonical approach, the cross-over line for chiral symmetry breaking has been calculated by minimizing the light quark mass susceptibility  $\chi_m$ . As has been mentioned, by forcing the location of the minimum to coincide with the fitted  $T$  and  $\mu_B$  in Pb–Pb collisions at  $\sqrt{s_{NN}} = 17.3 \text{ GeV}$ , we have been able to set the parameter  $T_0$  to 170 MeV (see Fig. 3). For this calculation, the u and d chemical potentials have been assumed to be equal, so that  $\chi_u$  and  $\chi_d$  coincide with  $\chi_m$ , whereas the strange quark chemical potential  $\mu_s$  has been set to zero due to  $S = 0$  constraint. It must be noted that, in principle,  $\mu_u$  and  $\mu_d$  differ because:

$$\begin{aligned}\mu_u &= \frac{\mu_B}{3} + \frac{2}{3}\mu_Q \\ \mu_d &= \frac{\mu_B}{3} - \frac{1}{3}\mu_Q \\ \mu_s &= \frac{\mu_B}{3} - \frac{1}{3}\mu_Q - \mu_S\end{aligned}\tag{21}$$

where  $\mu_Q$  is the electrical chemical potential, which vanishes only in isospin symmetric systems. However, this term turns out to be negligible for all examined collisions (see Table I) and we have simply taken  $\mu_u = \mu_d = \mu_B/3$ . Having set  $T_0$ , the cross-over curve can be predicted from the model and this is shown in Fig. 5 along with fitted SHM points which are in satisfactory agreement with the calculation.

It must be pointed out that in a grand-canonical finite system with fixed volume, the conservation of a definite initial values of baryon number, electric charge and strangeness necessarily leads to different values of the chemical potentials for the two different phases, such as the considered constituent quark phase and the hadron gas. Certainly, the volume is not supposed to be fixed in the transition, thus the assumption of equal  $\mu_B$ 's may be correct. On the other hand, once  $\mu_B$  has been set, the constraints  $S = 0$  and  $Q/B = Z/A$  lead to definite  $\mu_Q$  and  $\mu_S$  (beware the difference with  $\mu_s$ ) values which, in principle, are different in the two phases. While retaining  $\mu_s = 0$ , we have checked the accuracy of the assumption  $\mu_Q = 0$  by studying the effect on  $\lambda_S$  of non-vanishing electrical chemical potentials in the quark phase. The procedure is as follows: first, we have calculated  $\lambda_S$  and quark masses with the main assumption, i.e.  $\mu_Q = 0$ ; then, by using those masses, we have calculated  $\mu_Q$  in the quark phase by enforcing  $Q/B = Z/A$ ; finally, with the obtained  $\mu_Q$ , we have recalculated quark masses and the new  $\lambda_S$ . The difference between the  $\lambda_S$ 's calculated in the two ways ranges from 1% in Pb–Pb collisions at SPS energy up to 2.7% in Au–Au collisions at AGS energy and is therefore negligible throughout.

The parameter  $\lambda_S$  has been calculated along the cross-over curve by using Eq. (17) and the comparison with the SHM fitted values is shown in Fig. 6. The main prediction of the NJL-based model is an increase of  $\lambda_S$  for decreasing  $\sqrt{s}$  which is driven by the increase of  $\mu_B$  (see Table I). This involves an enhancement of relative strange quark production with respect to u, d, the so-called Pauli blocking effect. On the other hand, the observed  $\lambda_S$  does not keep growing but undergoes a dramatic drop at very small energies (see Fig. 1), a fact which can be possibly explained by the onset of a purely hadronic production mechanism at low (yet not easy to locate) center-of-mass energies with possible local strangeness conservation [35]. Looking at the deviations of the SHM-fitted central values of  $\lambda_S$  in Au–Au and Si–Au from the theoretical curve in Fig. (6), it can be argued that this hadronic production mechanism takes over at energies as low as AGS's. Certainly, error bars are large and a definite conclusion needs more precise data. It should also be pointed out that a mild strange canonical suppression sets in already in AGS Si–Au collisions[10] which is not taken into account here. Another sizeable discrepancy between data and model shows up in Au–Au collisions at RHIC ( $\sqrt{s} = 130 \text{ GeV}$ ). However, in this case,  $\lambda_S$  has been determined by fitting ratios of hadronic yields measured at mid-rapidity, unlike all other quoted collisions for which full phase space multiplicities have been used. This method may have led to an overestimation of  $\lambda_S$  if the midrapidity region is enriched in strangeness as observed in Pb–Pb collisions at SPS[36].

It is now worth discussing the robustness of these results in some detail. The calculation of  $\lambda_S$  based on Eq. (17) depends on constituent quark masses and the UV cutoff parameter  $\Lambda$  besides the thermodynamical parameters  $T$  and  $\mu_B$  which have been set by using hadronic fits. This expression of  $\lambda_S$  is indeed a general one for effective models with four fermion interactions in the mean-field approximation. It is then worth studying  $\lambda_S$  by taking the constituent

masses as free parameters instead of fixing them by means of a particular effective model as we have done so far. Whilst  $M_{u,d}(\mu, T)$  is strongly dependent on  $T_0$ ,  $M_s(\mu, T)$  is fairly independent of it (see Fig. 2). Therefore, as far as the finite temperature sector is concerned, one can fairly conclude that this NJL model has actually one free parameter, either  $T_0$  or  $M_{u,d}(\mu_{Bc}, T_c)$ . In other words, fixing  $T_0$  amounts to set a definite value of the light quark mass at the critical point.

However, the resulting  $\lambda_S$  value does not strongly depend on this parameter either, as shown in Fig. 7, where the region in the  $(M_u, M_s)$  plane (with both  $\Lambda = 631.4$  MeV and  $\Lambda = +\infty$ ) allowed by the fitted  $\lambda_S$  values in Pb–Pb collisions at  $\sqrt{s_{NN}} = 17.3$  GeV is shown: the bands pattern clearly indicates that  $\lambda_S$  has a strong dependence on  $M_s$  and much milder on  $M_{u,d}$ . Furthermore, the  $M_s$  value at the critical temperature is quite constrained by its corresponding value at zero temperature and does not undergo strong variations as a function of the temperature and  $T_0$ , as shown in Fig. (2), which is indeed a quite general feature of effective models [22]. Summarizing, we can state that this NJL model yields a  $\lambda_S$  value in good agreement with the data (as determined through the SHM) essentially because it has a fit value of the constituent strange quark mass at zero temperature and density (about 500 MeV), whilst the particular value of  $T_0$  has much less impact on it (see also Fig. (7)). On the other hand, for fixed constituent quark masses,  $\lambda_S$  is sizeably affected by the cutoff  $\Lambda$ . The calculation with  $\Lambda = +\infty$  is meant to give some upper bound on its variation due to neglected UV contributions, though a re-analysis within a renormalizable model would be desirable to have a more accurate estimation.

## B. Elementary collisions

In EC the fitted total volumes are small and the calculations have to be carried out within the canonical formalism. As has been mentioned in the previous section, the partition function to be used is that in Eq. (12) with constituent masses replacing current masses and a  $\Lambda$  cut-off as upper bound in the momentum integration in Eq. (6). Unlike in the grand-canonical ensemble,  $\lambda_S$  depends on the volume and a thorough comparison with SHM fitted parameters is much more involved. This is true in many respects: first, the fitted total volumes in the SHM are subject to large errors and obtained for point-like hadrons, thus reasonably underestimated. Secondly, for finite volumes one should in principle refit  $T_0$  so as to obtain a cross-over point for a definite total volume  $V$  and cluster volume  $V_c$ , for each process, at the desired temperature. Finally, one should minimize the full expression of free energy  $F = -T \log Z$  (with  $Z$  as in (12)) to determine the constituent masses at finite volume. For the present, this calculation is not affordable as the minimization of functions involving five-dimensional numerical integration as in Eq. (12) at each step with the due accuracy, implies exceedingly high computing times with presently available computers. For this reason, we have carried out a simpler calculation, with  $T_0$  kept to 170 MeV and constituent quark masses calculated in the model at the thermodynamic limit.

Yet, even in this approximated calculation, the effect of flavor and color conservation over finite volumes can be studied and, hopefully, it can be verified if this mechanism of canonical suppression actually implies a reduction of  $\lambda_S$  with respect to the thermodynamic limit consistently with the data. In fact, any conservation law enforced on finite volumes imply a reduction of heavy charged particle multiplicity stronger than lighter particles' so that a decrease of  $\lambda_S$  for decreasing volumes is expected. The ultimate reason of this effect is the reduced energy expense needed, in a finite system, to compensate any charge unbalance with light particles in comparison with heavy particles.

We can see this mechanism at play in Fig. 8 where  $\lambda_S$  is plotted as a function of the total volume  $V$  (over which flavor is exactly conserved), for different (color-singlet) cluster volumes  $V_c$  for an initially completely neutral system, such as  $e^+e^-$ . The temperature has been set to  $T = 160$  MeV, which is a fair average of the SHM fitted values [2, 12, 17] in  $e^+e^-$  and the constituent quark masses have been set to  $M_s = 452$  MeV and  $M_{u,d} = 112$  MeV, which are the thermodynamic limit values. Interestingly,  $\lambda_S$  features a fair stability over a large range of total volumes greater than  $\approx 20$  fm<sup>3</sup> for  $V_c < 10$  fm<sup>3</sup> within the data band, with a mild increase up to an asymptotic value which turns out to be closer to the thermodynamic limit (yet not equal to it, see also Fig. (4)) for larger  $V_c$ . As the volumes fitted in a point-like hadron gas model in  $e^+e^-$  and  $p\bar{p}$  collisions turn out to be larger than 15 fm<sup>3</sup>, but not larger than  $\simeq 80$  fm<sup>3</sup>, we can argue that a suitable  $V_c$  can account for the observed values and the stability of  $\lambda_S$  over a reasonably large volume range, taking into account that the actual volumes are certainly larger than their point-like estimates. Moreover, the mechanism of local color neutrality induces the reduction of  $\lambda_S$  value with respect to the thermodynamic limit of  $\simeq 0.31$  which is needed to quantitative reproduce the data. Within this approach, the difference between  $\lambda_S$  in high energy HIC and EC would be mainly the result of the non vanishing initial baryon density (from  $\simeq 0.31$  to  $\simeq 0.45$ ) and of local color neutrality in EC over small regions (5 – 10 fm<sup>3</sup>).

The situation is somewhat different for pp collisions, due to non vanishing initial baryon number and electric charge. In this system, one can observe two compensating effects, namely Pauli exclusion principle favoring relative  $s\bar{s}$  production and canonical suppression, favoring relative  $u\bar{u}$  and  $d\bar{d}$  production. As a result,  $\lambda_S$  is nearly constant around 0.3, in apparent disagreement with the observed value which is about 0.2 (see Fig. 9). The reduction of  $\lambda_S$



brought about by the decrease of  $V_c$  is not sufficient to restore the agreement even for very low  $V_c$ . The disagreement can be possibly explained by the inadequacy of the taken assumptions, such as the statistical distribution of charges among clusters according to Eq. (9).

## V. CONCLUSIONS AND OUTLOOK

We have presented a statistical model to explain the observed pattern of strangeness production in both elementary and heavy ion collisions. The basic idea is that full chemical equilibrium is locally achieved at the level of constituent quark degrees of freedom (within the framework of a simple effective model), at a different stage of the evolution process in elementary collisions (late) with respect to heavy ion collisions (early). In this approach, hadron formation takes place through the coalescence of constituent quarks and this accounts for the known observation of an incomplete strangeness equilibrium at hadron level in the statistical hadronization models. The underlying assumption is that at least the ratio  $s/u$  survives in the final hadrons.

Besides the effect of different initial excess of matter over antimatter, the smaller relative strangeness production in EC with respect to HIC has been related to the smaller overall system size and to color confinement over much smaller regions. Particularly, the existence of a characteristic cluster volume, roughly between 5 and 10 fm<sup>3</sup> and independent of center-of-mass energy, can possibly account for the observed stability of  $\lambda_S$ , along with the constancy of temperature and the weak dependence of  $\lambda_S$  itself on the total volume  $V$  (if not below  $\sim 60$  fm<sup>3</sup>), at least in  $e^+e^-$  and  $p\bar{p}$  collisions. However, the dependence of  $\lambda_S$  on cluster volume in HIC is so mild that it is not possible to use strangeness production to prove the formation of large color-neutral regions, i.e. color deconfinement.

The numerical analysis, carried out within an effective Nambu-Jona-Lasinio model, involved only one parameter to be adjusted which has been used to get the critical point agreeing with that fitted in Pb–Pb collisions. A satisfactory agreement with the data has been found in several heavy ion collisions and  $e^+e^-$ ,  $p\bar{p}$  collisions. Deviations have been found at low energy HIC, such as Au–Au and Si–Au at AGS, where the strangeness production mechanism could be predominantly driven by hadronic inelastic collisions. Furthermore, a significant discrepancy has been found in pp, which might be perhaps cured by taking a different scheme of quantum numbers distribution among the hadronizing clusters. It should be pointed out that the analysis in EC has been performed with some approximations as a full consistent treatment of the Nambu-Jona-Lasinio model for finite volumes is presently beyond our possibilities.

The model-dependence of our results has been discussed. We are reasonably confident that the obtained results are quite general and stable within non-renormalizable models with four-fermion interactions treated in the mean field approximation. The exploration of renormalizable effective model is under investigation.

## APPENDIX A

We want to prove that:

$$\sum_{\mathbf{Q}_1, \dots, \mathbf{Q}_N} \prod_{i=1}^N Z_i(\mathbf{Q}_i) \delta_{\mathbf{Q}, \Sigma_i \mathbf{Q}_i} \quad (22)$$

is the global partition function in Eq. (12), with  $Z_i$  as in Eq. (7), provided that all clusters have the same volume  $V_c$ . We will first prove it in the canonical framework, with each cluster having also the same temperature  $T$ . One can rewrite Eq. (22) by using Eq. (7) and the integral representation of the  $\delta_{\mathbf{Q}, \Sigma_i \mathbf{Q}_i}$  as:

$$\sum_{\mathbf{Q}_1, \dots, \mathbf{Q}_N} \left[ \prod_{j=1}^3 \int_{-\pi}^{\pi} \frac{d\phi_j}{2\pi} \right] e^{i\mathbf{Q} \cdot \phi - i \Sigma_i \mathbf{Q}_i \cdot \phi} \prod_{i=1}^N \left[ \prod_{j=1}^3 \int_{-\pi}^{\pi} \frac{d\phi_{ji}}{2\pi} \right] e^{i\mathbf{Q}_i \cdot \phi_i} \int d\mu(\theta_1, \theta_2) e^{V_c f(\theta_1, \theta_2, \phi_i)} \quad (23)$$

where  $\hat{Z}_i$  has been written in the simple form  $\exp[V_c f(\theta_1, \theta_2, \phi_i)]$  according to Eq. (6). It must be stressed that this expression of  $\hat{Z}$  is very general and does not depend on the Hamiltonian of the considered model. Moreover, the function  $f$  is the same for all clusters for it depends only on the temperature which has been assumed to be the same. We can now perform the summation over all  $\mathbf{Q}_i$  in Eq. (22) and get:

$$\sum_{\mathbf{Q}_1, \dots, \mathbf{Q}_N} e^{i \Sigma_i \mathbf{Q}_i \cdot (\phi_i - \phi)} = \prod_{i=1}^N (2\pi)^3 \delta^3(\phi - \phi_i) \quad (24)$$

so that the integration over  $\phi_{ji}$  in Eq. (22) can be easily performed and one is left with:

$$\left[ \prod_{j=1}^3 \int_{-\pi}^{\pi} \frac{d\phi_j}{2\pi} \right] e^{i\mathbf{Q} \cdot \phi} \prod_{i=1}^N \int d\mu(\theta_1, \theta_2) e^{V_c f(\theta_1, \theta_2, \phi)} \quad (25)$$

The integral over SU(3) group is the same for all clusters and Eq. (25) can then be written as:

$$\begin{aligned} & \left[ \prod_{j=1}^3 \int_{-\pi}^{\pi} \frac{d\phi_j}{2\pi} \right] e^{i\mathbf{Q} \cdot \phi} \left[ \int d\mu(\theta_1, \theta_2) e^{V_c f(\theta_1, \theta_2, \phi)} \right]^N \\ &= \left[ \prod_{j=1}^3 \int_{-\pi}^{\pi} \frac{d\phi_j}{2\pi} \right] e^{i\mathbf{Q} \cdot \phi} \left[ \int d\mu(\theta_1, \theta_2) \hat{Z}_i(\theta_1, \theta_2, \phi) \right]^{V/V_c} \end{aligned} \quad (26)$$

where  $V = \sum_i V_i = NV_c$ , which is equal to the right hand side of Eq. (12).

## APPENDIX B

We show that the configuration probabilities  $w(\mathbf{Q}_1, \dots, \mathbf{Q}_N)$  in Eq. (9) minimize the free energy of a system with volume  $V$  and temperature  $T$  which is split into  $N$  color-singlet clusters with volumes  $V_1, \dots, V_N$  such that  $\sum_i V_i = V$ . Let  $p$  be the full probability of a single state in this system and  $w$  the probability of a configuration  $(\mathbf{Q}_1, \dots, \mathbf{Q}_N)$ . Then:

$$p_{\text{state}} = w(\mathbf{Q}_1, \dots, \mathbf{Q}_N) \prod_{i=1}^N \frac{\exp(-E_i/T)}{Z_i(\mathbf{Q}_i)} \delta_{\mathbf{Q}_i, \mathbf{Q}_{i;s}} \delta_{\text{singlet}_i} \quad (27)$$

where  $Z_i$  is given by Eq. (7),  $E_i$  is the energy of a cluster,  $\mathbf{Q}_{i;s}$  is the vector of flavor quantum numbers of the state and  $\delta_{\text{singlet}_i}$  signifies the color singlet constraint on each cluster. The entropy reads:

$$\begin{aligned} S &= - \sum_{\text{states}} p \log p \\ &= - \sum_{\mathbf{Q}_1, \dots, \mathbf{Q}_N} \sum_{\text{states}_1} \dots \sum_{\text{states}_N} w(\mathbf{Q}_1, \dots, \mathbf{Q}_N) \prod_{i=1}^N \frac{e^{-E_i/T}}{Z_i(\mathbf{Q}_i)} \log w(\mathbf{Q}_1, \dots, \mathbf{Q}_N) \left[ \prod_{i=1}^N \frac{\exp(-E_i/T)}{Z_i(\mathbf{Q}_i)} \right] \end{aligned} \quad (28)$$

where the flavor and color constraint on each cluster are now implied in the sum over the states.

Eq. (28) can be worked out:

$$\begin{aligned} S &= - \sum_{\mathbf{Q}_1, \dots, \mathbf{Q}_N} \sum_{\text{states}_1} \dots \sum_{\text{states}_N} w(\mathbf{Q}_1, \dots, \mathbf{Q}_N) \prod_{i=1}^N \frac{e^{-E_i/T}}{Z_i(\mathbf{Q}_i)} \\ &\quad \times \left[ \log w(\mathbf{Q}_1, \dots, \mathbf{Q}_N) - \frac{E_i}{T} - \log \prod_{i=1}^N Z_i(\mathbf{Q}_i) \right] \\ &= \sum_{\mathbf{Q}_1, \dots, \mathbf{Q}_N} w(\mathbf{Q}_1, \dots, \mathbf{Q}_N) \left[ - \log w(\mathbf{Q}_1, \dots, \mathbf{Q}_N) + \frac{\sum_{i=1}^N \langle E_i \rangle_{(\mathbf{Q}_1, \dots, \mathbf{Q}_N)}}{T} + \log \prod_{i=1}^N Z_i(\mathbf{Q}_i) \right] \end{aligned} \quad (29)$$

where  $\sum_i \langle E_i \rangle_{(\mathbf{Q}_1, \dots, \mathbf{Q}_N)}$  is the average energy for the  $i^{\text{th}}$  cluster and a fixed configuration  $(\mathbf{Q}_1, \dots, \mathbf{Q}_N)$ . The total average energy of the system, to be identified with the internal energy  $U$ , evidently reads:

$$U = \sum_{\mathbf{Q}_1, \dots, \mathbf{Q}_N} w(\mathbf{Q}_1, \dots, \mathbf{Q}_N) \sum_{i=1}^N \langle E_i \rangle_{(\mathbf{Q}_1, \dots, \mathbf{Q}_N)} \quad (30)$$

so that entropy can be rewritten as:

$$S = \sum_{\mathbf{Q}_1, \dots, \mathbf{Q}_N} -w(\mathbf{Q}_1, \dots, \mathbf{Q}_N) \log w(\mathbf{Q}_1, \dots, \mathbf{Q}_N) + \frac{U}{T} + \sum_{\mathbf{Q}_1, \dots, \mathbf{Q}_N} w(\mathbf{Q}_1, \dots, \mathbf{Q}_N) \log \prod_{i=1}^N Z_i(\mathbf{Q}_i) \quad (31)$$

and the free energy  $F$  as:

$$F = U - TS = T \sum_{\mathbf{Q}_1, \dots, \mathbf{Q}_N} w(\mathbf{Q}_1, \dots, \mathbf{Q}_N) \left[ \log w(\mathbf{Q}_1, \dots, \mathbf{Q}_N) - \log \prod_{i=1}^N Z_i(\mathbf{Q}_i) \right] \quad (32)$$

Now we seek for the probabilities  $w$  which minimize the free energy with the constraint  $\sum w = 1$ . Therefore we have to introduce a Lagrange multiplier  $\lambda$  and look for the extremals of  $F + \lambda(\sum w - 1)$  with respect to each  $w(\mathbf{Q}_1, \dots, \mathbf{Q}_N)$  and  $\lambda$ . This leads to:

$$\log w(\mathbf{Q}_1, \dots, \mathbf{Q}_N) = \log \prod_{i=1}^N Z_i(\mathbf{Q}_i) - \frac{\lambda}{T} \quad (33)$$

and

$$w(\mathbf{Q}_1, \dots, \mathbf{Q}_N) = \frac{\prod_{i=1}^N Z_i(\mathbf{Q}_i) \delta_{\mathbf{Q}, \Sigma_i \mathbf{Q}_i}}{\sum_{\mathbf{Q}_1, \dots, \mathbf{Q}_N} \prod_{i=1}^N Z_i(\mathbf{Q}_i) \delta_{\mathbf{Q}, \Sigma_i \mathbf{Q}_i}} \quad (34)$$

after proper normalization.

### Acknowledgments

We are grateful to J. Aichelin, A. Barducci, R. Casalbuoni, U. Heinz, J. Lenaghan, O. Scavenius for useful discussions.

- 
- [1] F. Becattini, Z.Phys. **C69**, (1996) 485.
  - [2] F. Becattini, in Proc. of “Universality features of multihadronic production and the leading effect”, October 19-25 1996, World Scientific p. 74, hep-ph 9701275; F.Becattini and U.Heinz, Z.Phys. **C76**, (1997) 269.
  - [3] E. Fermi, Progr. Theor. Phys. **5** (1950) 570.
  - [4] R. Hagedorn, N. Cim. Suppl. **3** (1965) 147.
  - [5] U. Heinz, Nucl. Phys. **A661** (1999) 140.
  - [6] R. Stock, Phys. Lett. **B456** (1999) 277.
  - [7] R. Hagedorn, CERN lectures “Thermodynamics of strong interactions” (1970) 46.
  - [8] see for instance: P. Braun-Munzinger et al., Phys. Lett. **B344** (1995) 43; P. Braun-Munzinger et al., Phys. Lett. **B365** (1996) 1; J. Cleymans et al., Z. Phys. **C74** (1997) 319; J. Cleymans et al., Phys. Rev. **C59** (1999) 1663; W. Florkowski et al., Acta Phys. Polon. **B33** (2002) 761.
  - [9] F. Becattini, J. Cleymans, A. Keranen, E. Suhonen, K. Redlich, Phys. Rev. **C64** 024901.
  - [10] F. Becattini, M. Gazdzicki and J. Sollfrank, Eur. Phys. J. **C5** (1998) 143.
  - [11] S. Bass, A. Dumitru et al., Phys. Rev. **C60** (1999) 021902.
  - [12] F. Becattini, G. Passaleva, Eur. Phys. J. **C23** (2002) 551.
  - [13] P. Rehberg and J. Aichelin, Phys. Rev. **C60** (1999) 064905.
  - [14] O. Scavenius, A. Dumitru, J. Lenaghan, hep-ph/0201079. Phys. Rev. **D38**, (1988) 238.
  - [15] A. Barducci, R. Casalbuoni, S. De Curtis, R. Gatto and G. Pettini, Phys. Lett. **B244**, (1990) 311.
  - [16] F. Karsch and E. Laermann, Phys. Rev. **D59** (1999) 031501; F. Karsch hep-lat/9903031.
  - [17] For a review see: F. Becattini, “Statistical hadronisation phenomenology”, talk given in Statistical QCD, Bielefeld, Aug. 25-30 2001.
  - [18] Y. Nambu, G. Jona-Lasinio, Phys. Rev. **122**, (1991) 345 and Phys. Rev. **124**, (1991) 246.
  - [19] T. Hatsuda and T. Kunihiro, Phys. Rep. **247**, (1994) 221.
  - [20] A. Barducci, R. Casalbuoni, S. De Curtis, D. Dominici and R. Gatto,

- [21] A. Barducci, R. Casalbuoni, S. De Curtis, R. Gatto and G. Pettini, Phys. Lett. **B231**, (1989) 463; Phys. Rev. **D41**, (1990) 1610; Phys. Rev. **D46**, (1992) 2203.
- [22] A. Barducci, R. Casalbuoni, R. Gatto and G. Pettini, Phys.Rev. **D49**, (1994) 426.
- [23] O. Kiriya, M. Maruyama and F. Takagi, Phys.Rev. **D63** (2001) 116009.
- [24] Z. Fodor, hep-lat 0209101 and references therein.
- [25] T.M. Schwarz, S.P. Klevansky and G. Papp Phys.Rev.**C60** (1999) 055205.
- [26] see for instance: F. Gastineau, R. Nebauer and J. Aichelin, Phys. Rev. **C65**,(2002) 045204.
- [27] G. Alford, K. Rajagopal and F. Wilczek, Nucl.Phys. **B422** (1998) 247 and Nucl.Phys. **B537** (1999) 443; J. Berges, K. Rajagopal, Nucl.Phys. **B538** (1999) 215.
- [28] J. Rafelski and B. Muller, Phys. Rev. Lett. **48** (1982) 1066.
- [29] K. Redlich and L. Turko, Z.Phys. **C5**, (1980) 201; L. Turko,Phys.Lett. **104B**, (1981) 153; M.I. Gorenstein, S.I. Lipskikh, V.K. Petrov and G.M. Zinovjev, Phys. Lett. 123B, (1983) 437; M.I. Gorenstein, O.A. Mogilevsky, V.K. Petrov and G.M. Zinovjev, Z. Phys. **C18**, (1983) 13; G. Auberson, L. Epele, G. Mahoux and F.R.A. Simao, J.Math.Phys. **27** (6), (1986) 1658.
- [30] M. Kobayashi and T. Maskawa, Prog.Theor.Phys. **44**, (1970) 1422; M. Kobayashi, H. Kondo and T. Maskawa, Prog.Theor.Phys. **45**, (1971) 1955; G. 'tHooft, Phys.Rev. **D14**, (1976) 3432; Phys.Rep. **142**, (1986) 357; M.A. Shifman, A.I. Vainshtein and V.Z. Zakharov, Nucl.Phys. **163B**, (1980) 46.
- [31] R. Jackiw, Phys.Rev. **D9**, (1974) 1686; J.M. Cornwall, R. Jackiw and E. Tomboulis, Phys.Rev. **D10**, (1974) 2428.
- [32] L. Dolan and R. Jackiw, Phys. Rev. **D9**, (1974) 3320; C.W. Bernard, Phys.Rev. **D9**, (1974) 3312.
- [33] see for instance: V.A. Miransky, "Dynamical Symmetry Breaking In Quantum Field Theories", World Scientific (1993), and references therein.
- [34] A. Keranen, F. Becattini, Phys. Rev. **C65** (2002) 044901.
- [35] S. Hamieh, K. Redlich and A. Tounsi, Phys. Lett. **B486** (2000) 61.
- [36] F. Becattini, talk given at "Strange Quarks in Matter 2001", J. Phys. **G28** (2002) 1553.
- [37] P. Braun-Munzinger et al., Phys. Lett. **B518** (2001) 41.

TABLE I: Parameters determined through statistical model fits to measured multiplicities in some elementary and heavy ion collisions. Heavy ion parameters have been taken from refs. [9, 36] whilst elementary collisions from refs. [2, 12];  $e^+e^-$  at  $\sqrt{s} = 91.2$  and  $p\bar{p}$  points have been refitted with updated data and hadronic input parameters. The  $pp$  point has been fitted with a different parametrization of the strangeness suppression [12] and  $\gamma_S$  has been replaced with the mean value of strange quark pairs  $\langle s\bar{s} \rangle$ ; the corresponding  $\gamma_S$  would be  $\simeq 0.5$ . The numerical values in Pb-Pb at  $\sqrt{s} = 8.7$  GeV have been obtained in ref. [36] with preliminary data from experiment NA49, those in Au-Au collisions at  $\sqrt{s} = 130$  GeV from a numerical analysis of midrapidity ratios as quoted in ref. [37]. The quoted central values of volumes (the volume is defined as the sum of the volumes of all produced clusters), have been obtained with pointlike hadrons, thus they must be taken as lower limits for the actual values. The errors on volumes, not quoted here, are generally large and can be up to 50%. Also quoted the central values of the electrical chemical potentials obtained in heavy ion collisions.

Collision	$\sqrt{s}$ (GeV)	$T$ (MeV)	$\mu_B$ (MeV)	$\gamma_S$	$\lambda_S$	$\mu_Q$ (MeV)	$V$ (fm <sup>3</sup> )
Au-Au	130	167±7.2	45.8±6.4	1.04±0.10	0.476±0.049	-1.42	-
Pb-Pb	17.3	158.1±3.2	238±13	0.789±0.0582	0.447±0.025	-6.87	3460
Pb-Pb	8.7	149.0±2.4	393.7±8.3	0.822±0.058	0.585±0.052	-11.2	2067
Si-Au	5.4	133.4±4.3	581±32	0.845±0.101	0.72±0.14	-10.7	330
Au-Au	4.8	121.2±4.9	559±16	0.697±0.091	0.43±0.10	-12.4	2805
$e^+e^-$	14	167.4±6.5		0.795±0.088	0.243±0.036		15.9
$e^+e^-$	91	159.2±0.8		0.664±0.014	0.225±0.004		52.4
$pp$	27.4	162.4±1.6		$\langle s\bar{s} \rangle$ 0.653±0.017	0.201±0.005		25.5
$p\bar{p}$	200	175±11		0.491±0.056	0.214±0.025		35.5
$p\bar{p}$	900	167.±9.0		0.533±0.054	0.230±0.033		77.3

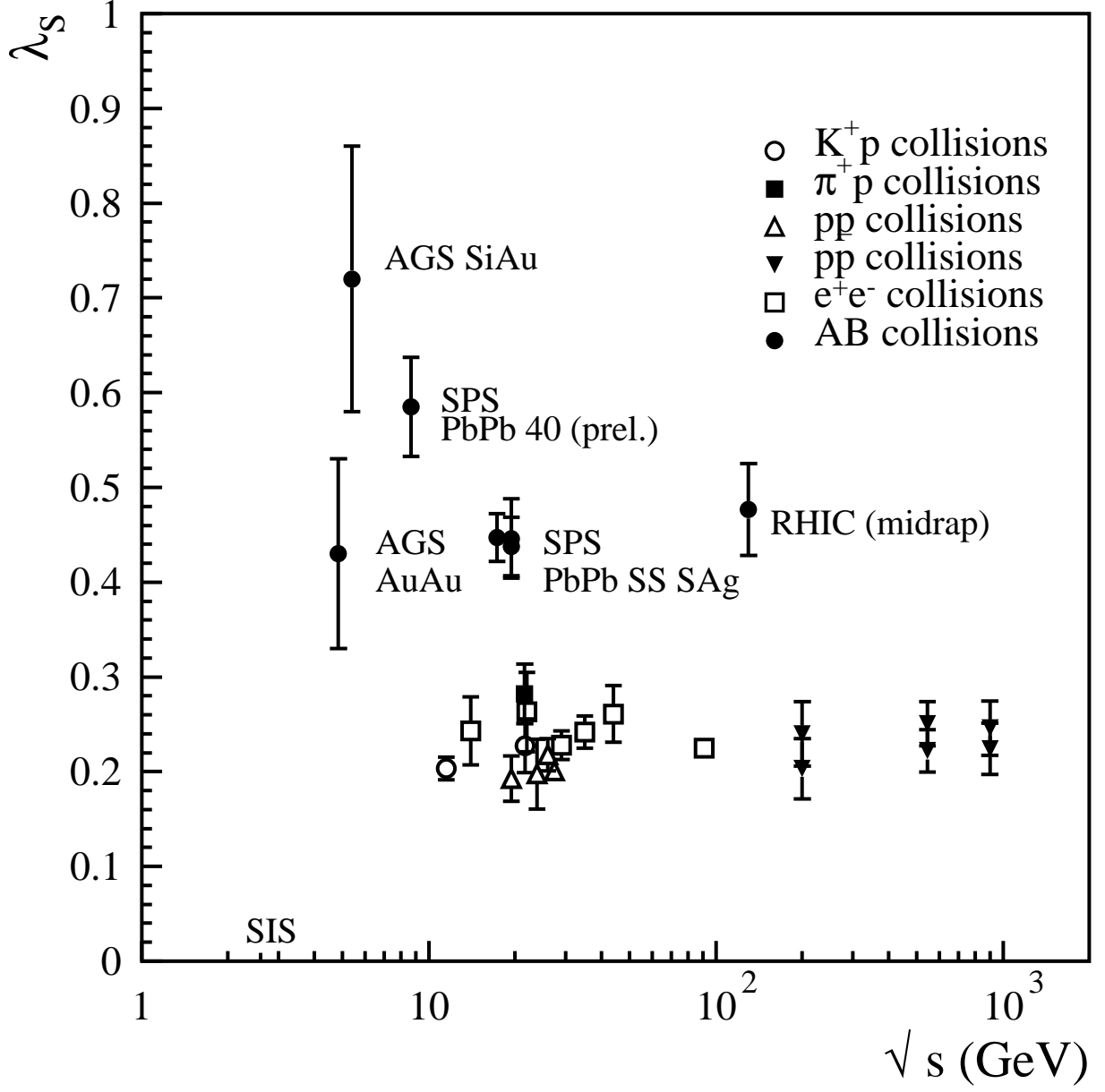
FIG. 1:  $\lambda_S$  in various elementary and heavy ion collisions (from [36]).

FIG. 2: Constituent masses of the quark  $s$  and the light quarks  $u, d$  as a function of temperature, with fixed  $\mu_{u,d}/T = 0.5$  and  $\mu_s = 0$ . The three curves correspond to different  $T_0$  values. The vertical lines define the  $1\sigma$  band for Pb-Pb collisions at  $\sqrt{s_{NN}} = 17.3$  GeV, as fitted in the SHM [9].

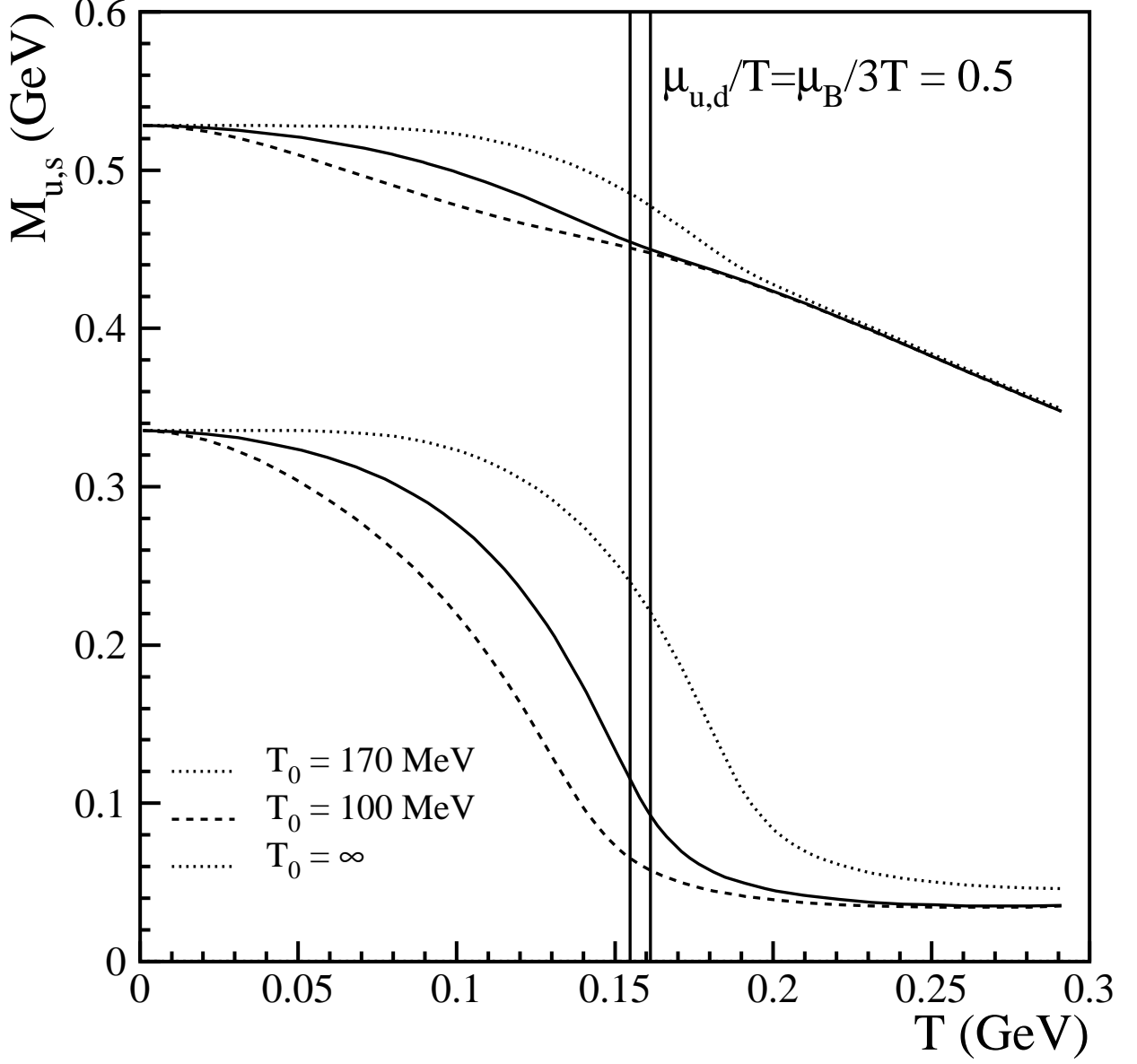


FIG. 3: Chiral susceptibility  $\chi_m$  for the quark u or d with current mass 5.5 MeV as a function of temperature  $T$ , for different values of the  $T_0$  parameter in the NJL model. The baryon chemical potential  $\mu_B$  has been set to 238 MeV and  $\mu_Q$  has been set to 0, in accordance with the analysis of full phase space Pb–Pb data at SPS energy [9]. The maximum of  $-\chi_m$  is located at  $T = 158$  MeV, the fitted value in Pb–Pb collisions at SPS energy for  $T_0 = 170$  MeV.

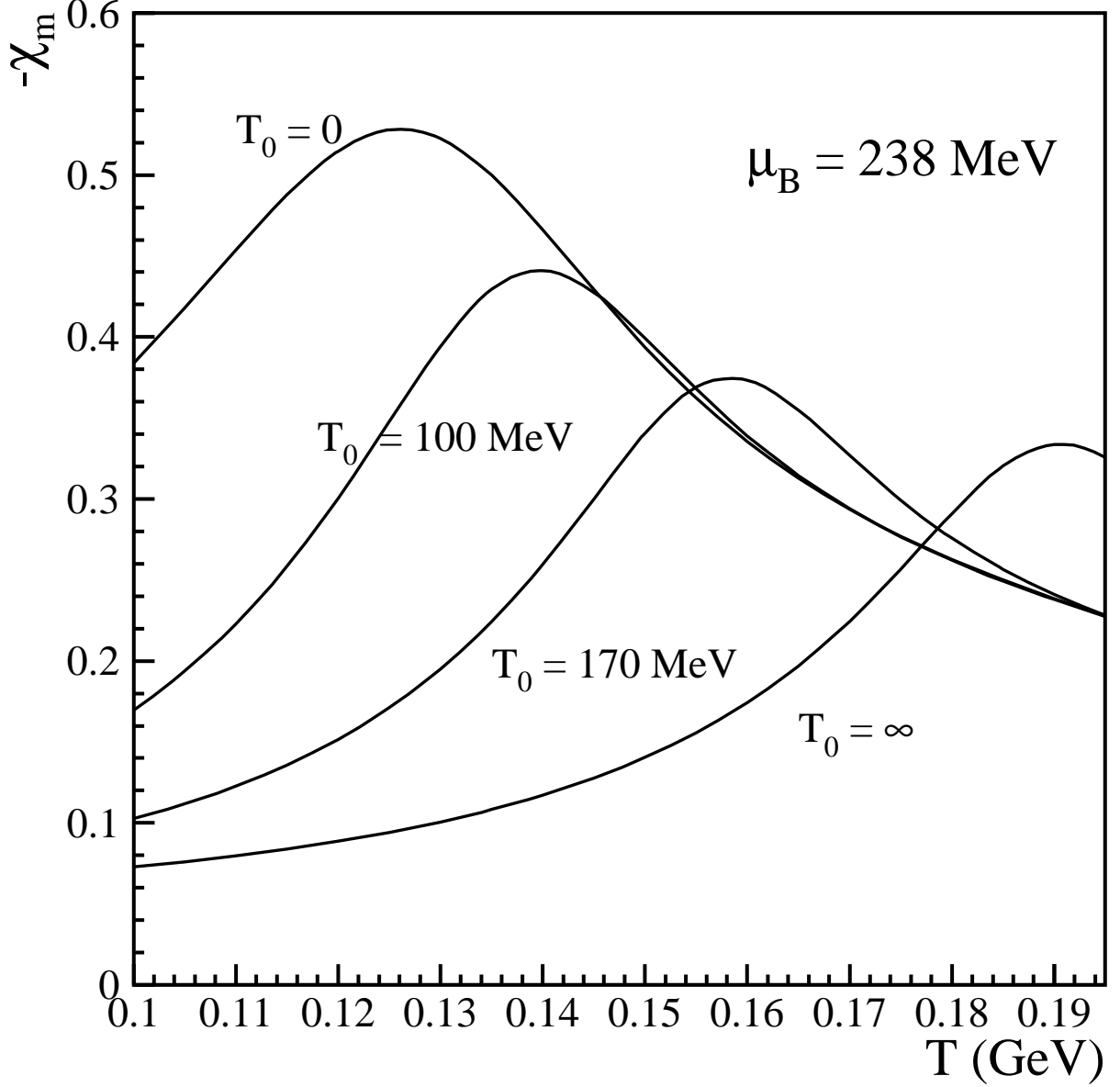




FIG. 4: Calculated  $\lambda_S$  in the NJL model in a color singlet cluster with  $T = 158$  MeV, baryon chemical potential  $\mu_B/T = 1.5$ ,  $\mu_Q = 0$  and  $\mu_s = 0$ , as a function of the volume. The dashed line indicates the grand-canonical value of  $\lambda_S$ . The constituent quark masses have been fixed to their values in the grand-canonical limit:  $M_u = M_d = 103$  MeV and  $M_s = 452$  MeV.

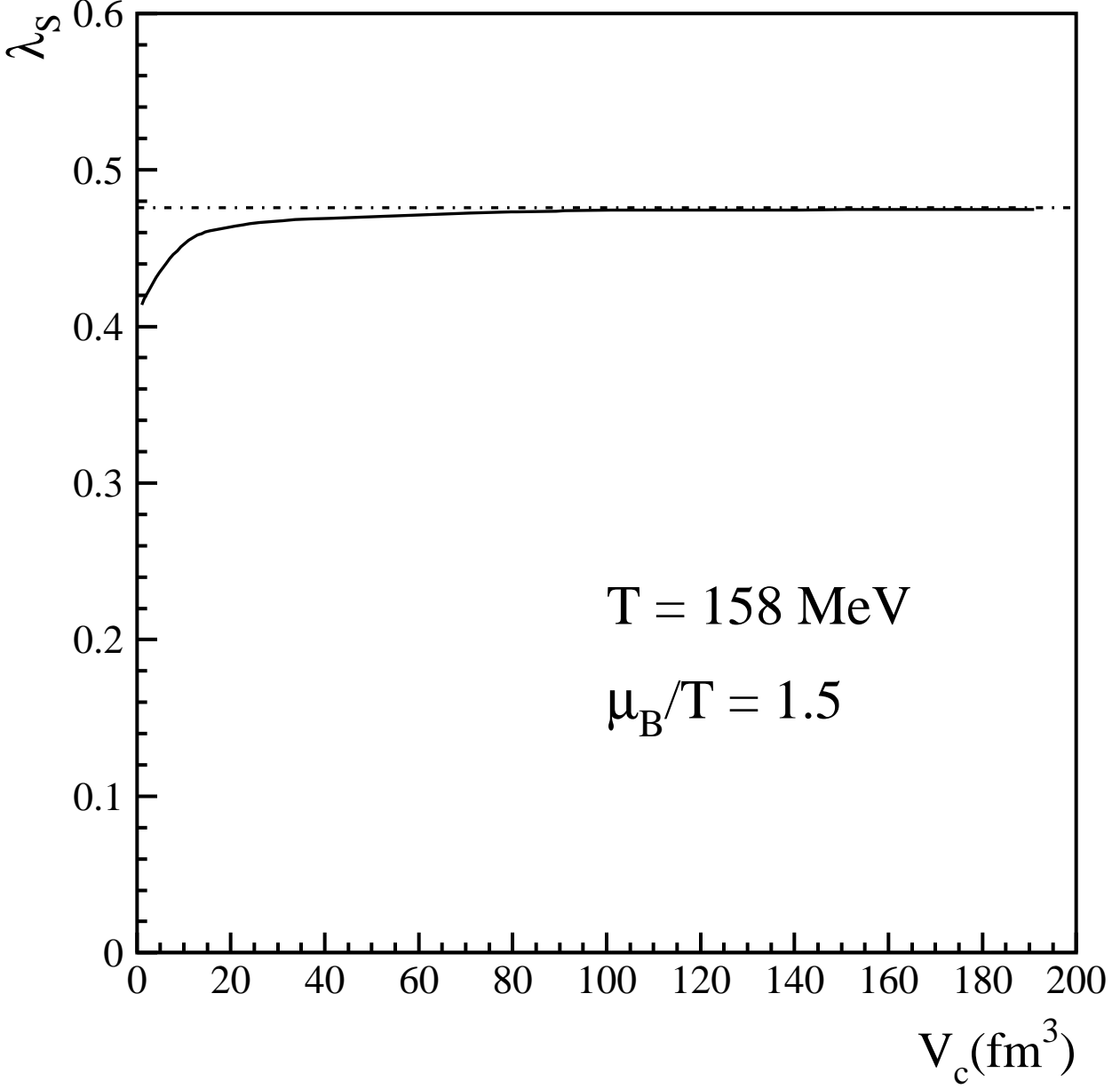


FIG. 5: Cross-over curve in the NJL model with  $T_0 = 170$  MeV in the  $(\mu_B, T)$  plane. Black dots with error bars are the values obtained within the SHM analysis in various heavy ion reactions [9],[36].

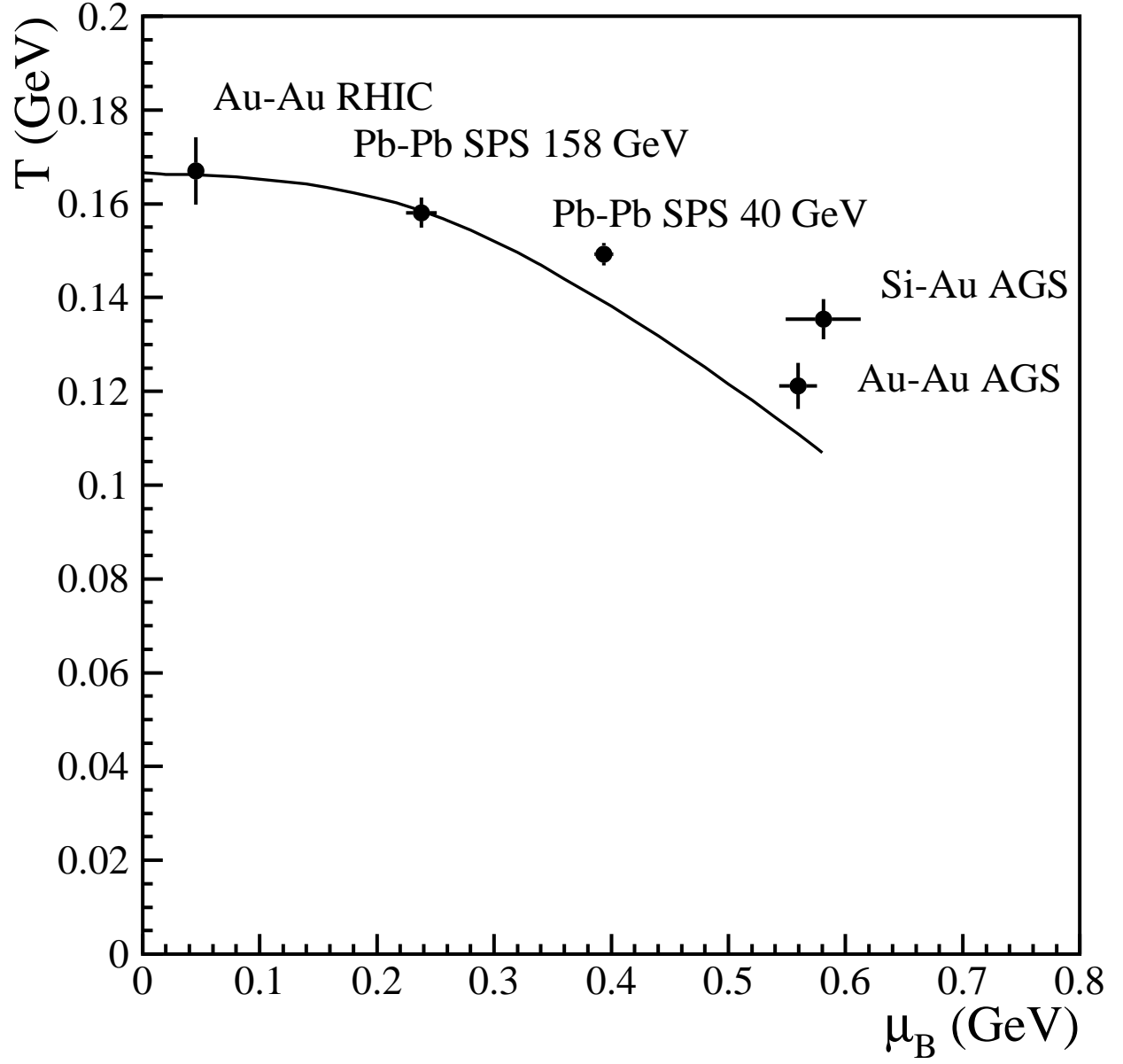


FIG. 6:  $\lambda_S$  calculated along the cross-over curve predicted in the NJL model with  $T_0 = 170$  MeV. Black dots with error bars are the values obtained within the SHM analysis in various heavy ion reactions [9, 36].

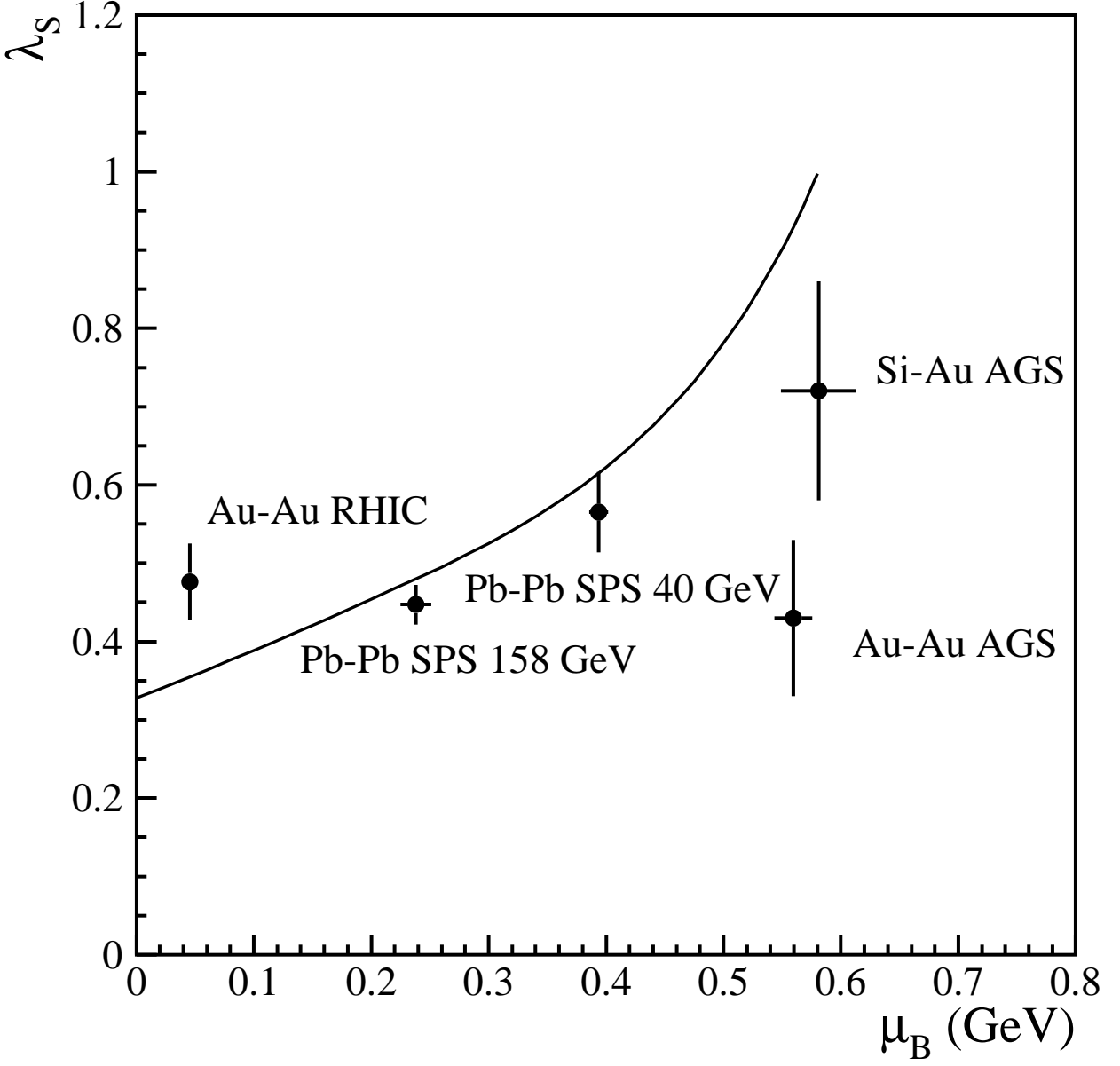


FIG. 7: Allowed regions of constituent quark masses  $M_{u,d}, M_s$  determined by the parameters  $\lambda_S = 0.447 \pm 0.025$ ,  $T = 158.1 \pm 2.3$  and  $\mu_B = 238 \pm 13$  MeV as fitted in Pb-Pb collisions at  $\sqrt{s_{NN}} = 17.3$  GeV [9], with  $\mu_Q = 0$  and  $\mu_s = 0$ . The lighter hatched region corresponds to the  $\Lambda$  momentum cut-off as in the NJL model [19] whereas the hatched darker region to the free constituent quark gas (i.e.  $\Lambda = \infty$ ). The solid line shows the predictions of the full NJL model with  $T_0$  ranging from zero (no KMT term) to  $\infty$  (CASE I in ref. [19]) from left to right, in the grand-canonical ensemble with  $T = 158.1$  MeV and  $\mu_B = 238$  MeV while the black dot shows the values of masses for  $T_0 = 170$  MeV. The dash-dotted horizontal and vertical lines correspond to the  $T = \mu_B = 0$  constituent masses values for the strange quark and for the light quarks u,d respectively.

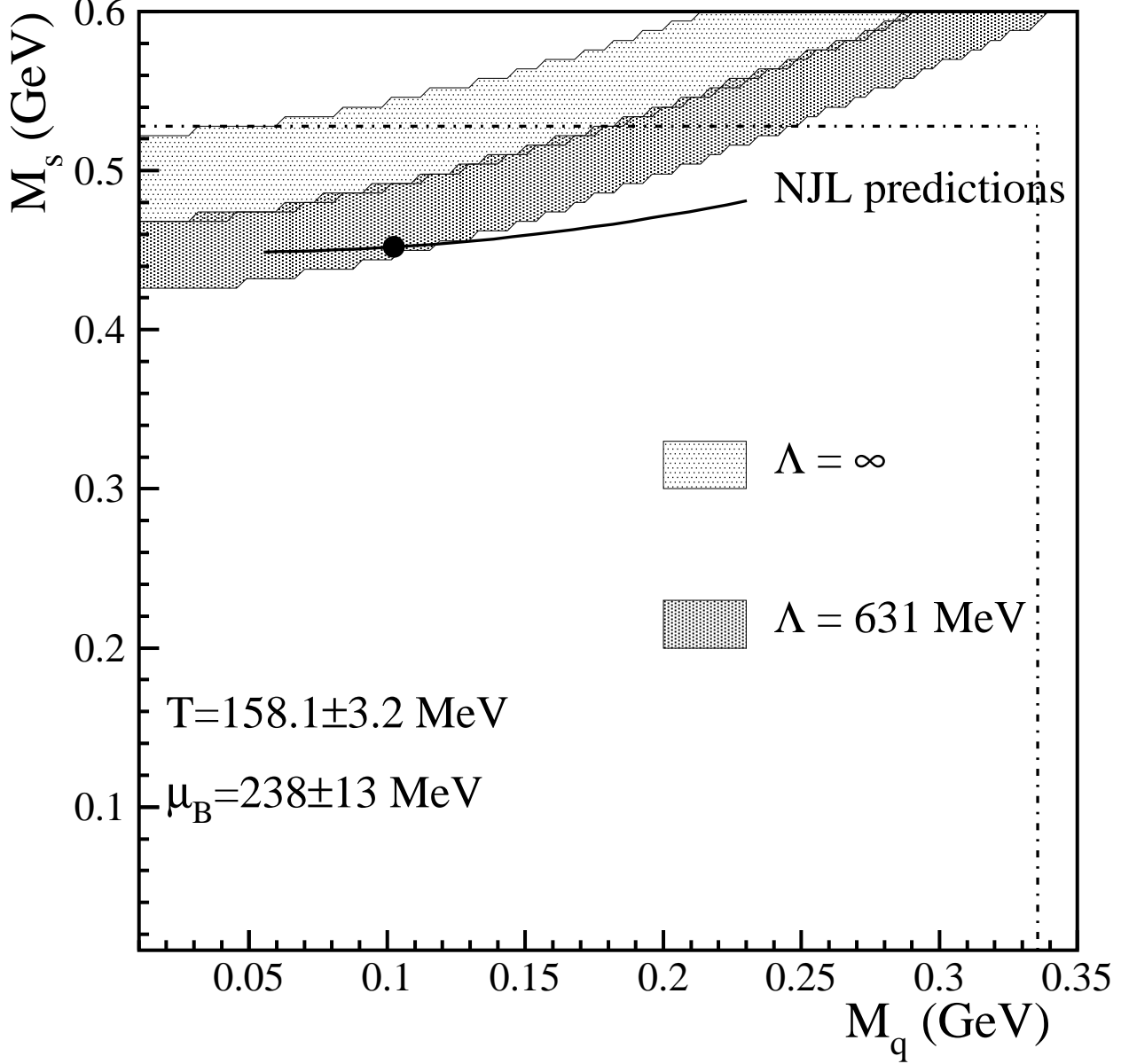


FIG. 8: Plot of  $\lambda_S$  as a function of the total volume  $V$  of the hadronizing clusters, for various (color singlet) single cluster volumes  $V_c$  in an initially completely neutral system. The constituent quark masses have been set to their values obtained in the grand-canonical case with  $T = 160$  MeV and all chemical potentials vanishing. The dotted line has been obtained by disregarding the color singlet constraint and keeping only the flavor constraint, for a given volume. The arrow indicates the asymptotic value in the grand-canonical limit. The horizontal band is the region determined by the maximal spread of central values obtained in the SHM fits in  $e^+e^-$  [2, 12, 17] and in  $p\bar{p}$  collisions [2].

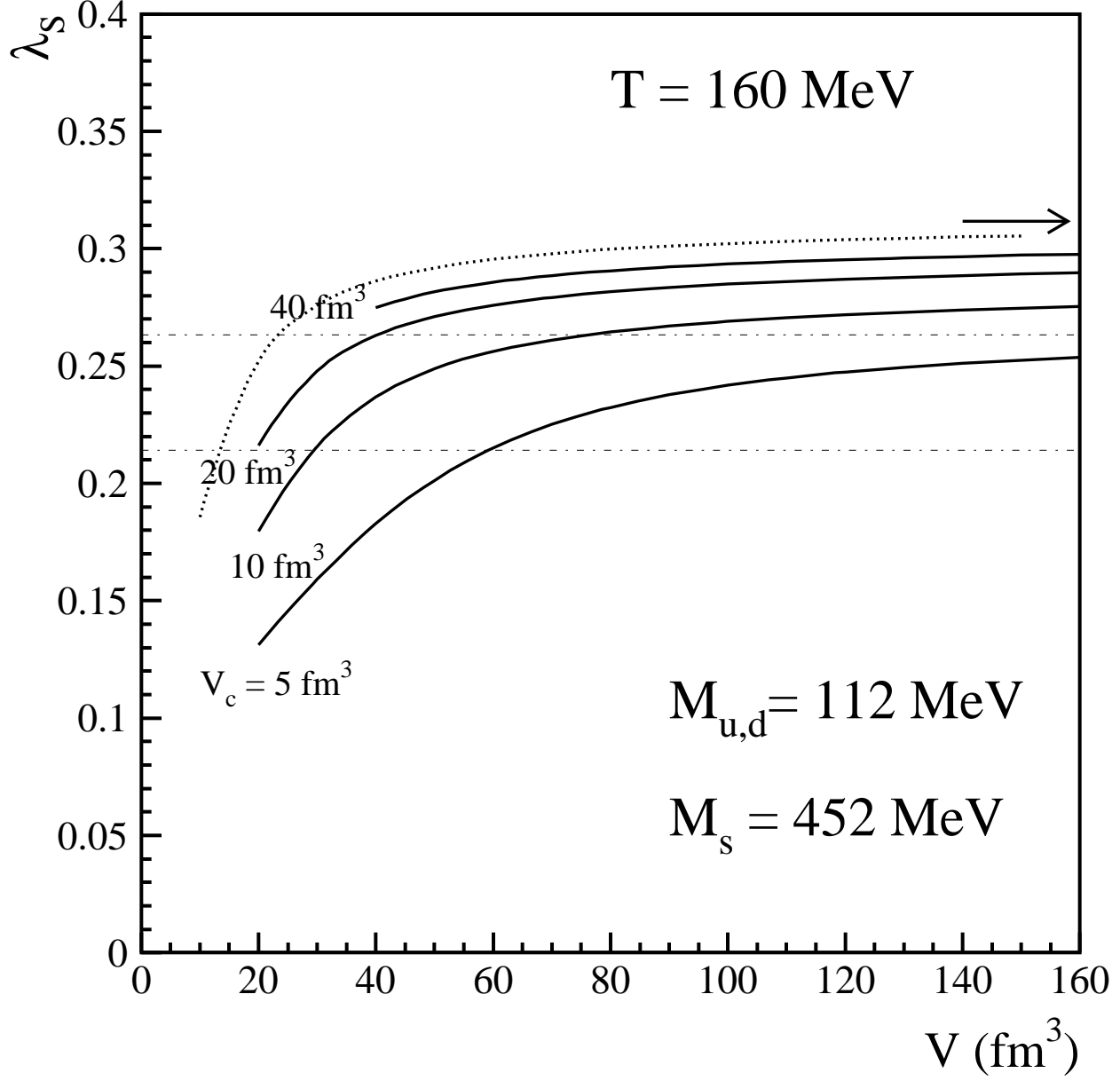


FIG. 9: Plot of  $\lambda_S$  as a function of the total volume  $V$  of the hadronizing clusters, for various (color singlet) single cluster volumes  $V_c$  in an initially pp-like system ( $B = Q = 2$ ,  $S = 0$ ). The constituent quark masses have been set to their values obtained in the grand-canonical case with  $T = 160$  MeV and all chemical potentials vanishing. The dotted line has been obtained by disregarding the color singlet constraint and keeping only the flavor constraint, for a given volume. The arrow indicates the asymptotic value in the grand-canonical limit. The horizontal band is the region determined by the maximal spread of central values obtained in the SHM fits in pp collisions [2, 12].

